Zeng Dezhi
State Key Laboratory of Oil and Gas Reservoir Geology and Exploitation, Southwest Petroleum University, Chengdu, Sichuan 610500, China; CNPC Key Lab for Tubular Goods Engineering, Southwest Petroleum University, Chengdu, Sichuan 610500, China

Deng Kuanhai
CNPC Key Lab for Tubular Goods Engineering, Southwest Petroleum University, Chengdu, Sichuan 610500, China

Shi Taihe
State Key Laboratory of Oil and Gas Reservoir Geology and Exploitation, Southwest Petroleum University, Chengdu, Sichuan 610500, China

Lin Yuanhua
State Key Laboratory of Oil and Gas Reservoir Geology and Exploitation, Southwest Petroleum University, Chengdu, Sichuan 610500, China
e-mail: yhlin28@163.com

Zhu Hongjun
CNPC Key Lab for Tubular Goods Engineering, Southwest Petroleum University, Chengdu, Sichuan 610500, China

Li Tianlei
China Petroleum Engineering Co., Ltd., Southwest Company, Chengdu, Sichuan 610017, China

Sun Yongxing
Drilling and Production Engineering Technology Research Institute (CCDC), Guanghan, Sichuan 618300, China

Theoretical and Experimental Study of Bimetal-Pipe Hydroforming

The corrosion of oil country tubular goods (OCTG) gets more and more serious especially in the acidic environment. So, it is very important to develop a perfect anticorrosion technology for exploring sour oil and gas fields economically and safely. Analysis indicates that the bimetal-pipe (BP) which consists of the base layer of low carbon steel and a corrosion resistant alloy (CRA) cladding layer is an economic and reliable anticorrosion technology and has broad application prospects in the transportation of acid medium. However, theoretical study of hydraulic expansion mechanism for BP is not enough. In this paper, the deformation compatibility condition of BP was obtained by studying the deformation rule of the (CRA) liner and the outer pipe of carbon steel in the forming process; the mechanical model which can compute the hydroforming pressure of BP has been established based on the nonlinear kinematic hardening characteristics of material; furthermore, based on the stress strain curve of inner pipe simultaneously, the calculation method of the plastic hardening stress has been proposed. Thus, the accurate method for computing the forming pressure was obtained. The experimental data show that results are consistent with results of the proposed model. It indicates that the model can be used to provide theoretical guidance for the design and production as well as use of BP. [DOI: 10.1115/1.4026976]

Keywords: bimetal-pipe, deformation compatibility condition, the nonlinear kinematic hardening characteristics of material, mechanical model, hydraulic forming experiment

1 Introduction

With the exploration and development of oil and gas, acidic gas reservoirs have to become the replacing resources. It makes the corrosive environment which OCTG is exposed to become more and more serious, such as high carbon dioxide, hydrogen sulfide and sulfur [1–4], etc., so the problem of oil pipe corrosion, paraffin and scaling of oil pipe gets more and more remarkable. It directly affects the economic benefit and safety of oil and gas field. In order to solve these problems, many anticorrosion technologies have been proposed such as corrosion inhibitor, plastic internal coating, CRA, and so on [5–14] in all over the world. Analyses indicates that BP which consists of the base layer of low carbon steel and a CRA cladding layer is an economic and reliable anticorrosion technology. So, BP was widely used in the oil and gas industry, such as the Fairwei oilfield in Mexico Bay in USA and the Buzzard field offshore the UK [15,16], etc. Due to high reliability and good economic benefits of BP, a large number of scholars have done a lot of studies about BP.

These studies mainly include the production technique and method [17–26] of BP, such as gas tungsten arc welding, pulse Rapid Arc gas metal arc welding of the pipes, reactive centrifugal casting method, explosive bonding, hot co-extrusion bonding, and hydraulic expansion of a CRA pipe inside and an outer pipe of carbon steel, etc., the theoretical researches about hydroforming processes of single metal tube [27–29], corrosion resistance of BP in nearly neutral aqueous media[30], the finite element analysis about hydroforming processes of BP were also studied [31,32]. However, the literatures about hydroforming processes on BP are little and the typical one is Wang's study [33] about hydroforming processes of BP. In Wang's study, the inner pipe is considered as linear hardening material and the nonlinear kinematic hardening characteristics of material was not taken into account, so that Wang's method has some disadvantages. In addition, Wang's method is not practical because the hardening modulus is difficult to know during the forming pressure calculation.

For the purpose of perfecting, the study about hydroforming processes of BP, in this paper, the deformation compatibility condition of BP was obtained by studying the deformation rule of the (CRA) liner and the outer pipe of carbon steel in the forming process; the mechanical model which can compute the hydroforming pressure of BP has been established based on the nonlinear

Contributed by the Pressure Vessel and Piping Division of ASME for publication in the Journal of Pressure Vessel Technology. Manuscript received December 30, 2012; final manuscript received February 12, 2014; published online September 4, 2014. Assoc. Editor: Roman Motriuk.

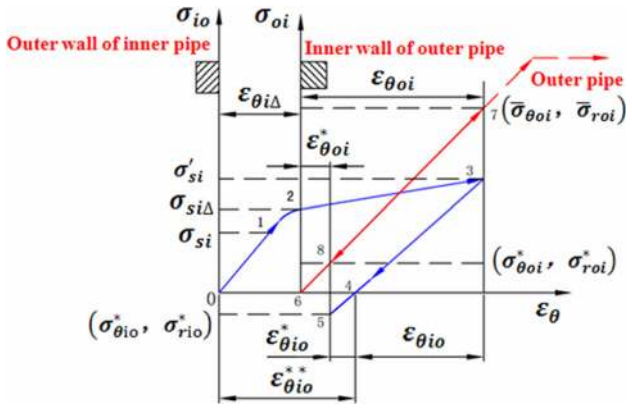

Fig. 1 The stress strain state characteristic and the correlation between stress and strain of BP in the forming process

kinematic hardening characteristics of material; furthermore, based on the stress strain curve of inner pipe simultaneously, the calculation method of the plastic hardening stress has been proposed. Thus, the accurate method for computing the forming pressure was obtained. The experimental data show that results are consistent with results of the model which indicates that the model can be used to provide theoretical guidance for the design and production as well as use of BP.

2 Theoretical Study of Hydraulic Forming Process for Bimetal-Pipe

2.1 The Deformation Compatibility Correlation in the Forming Process of BP. In order to make the usability of outer pipe remain unchanged, the internal pressure imposed on outer pipe cannot be greater than internal pressure strength of the outer pipe. Hence, only elastic deformation of outer pipe is produced in the forming process of BP. Therefore, the plastic deformation of outer pipe was not discussed in hydraulic forming process of BP. In order to analyze deformation compatibility condition of BP in hydraulic forming process visually, a relationship curve between the circumferential strain of inner and outer pipe, the stress of inner and outer pipe was plotted, as shown in Fig. 1.

It is obvious that the plastic deformation of inner pipe occurs and the elastic of the outer pipe occurs in the forming process. The bonding stress is equal to zero, and inner pipe and outer pipe just contact when the rebound of inner pipe is equal to the rebound of outer pipe after unloading. For the purpose of achieving formation, the forming pressure should be larger and larger so that the bonding stress between the inner pipe and outer pipe is produced. The stress and strain curve in the forming process is shown in Fig. 1.

In Fig. 1, the stress strain curve of inner pipe's outer wall has an origin (0, 0) and the stress strain curve of outer pipe's inner wall has an origin (6, 0). The stress path of inner pipe's outer wall is 0→1→2→3→4→5 and the stress path of outer pipe's inner wall is 6→8→7→8. From Fig. 1, it is known that when the stress of inner pipe's outer wall is equal to σ_{si}, the inner pipe begin to yield with the increase of forming pressure. When inner pipe's outer wall is equal to $\sigma_{si\Delta}$, the clearance (Δ) between the inner and outer pipe was eliminated and the circumferential strain of inner pipe's outer wall is $\varepsilon_{\theta i\Delta}$. When the elastic deformation of outer pipe' inner wall occurs, the stress state of outer pipe' inner wall can be obtained by point 6. The stress of inner pipe is strengthened and equal to σ'_{si}, when the load increase to point 3. At that moment, the radial and circumferential stresses of outer pipe' inner wall are $\bar{\sigma}_{\theta oi}$ and $\bar{\sigma}_{\theta oi}$, respectively, as shown at point 7. When the forming pressure was unloaded at point 7, the stress σ'_{si} and strain $\varepsilon_{\theta io}$ of inner pipe's outer wall should be eliminated. The stress ($\bar{\sigma}_{\theta oi}$, $\bar{\sigma}_{\theta oi}$) and strain $\varepsilon_{\theta oi}$ of outer pipe's inner wall should be eliminated. From Fig. 1, it is known that $\varepsilon_{\theta oi}$ is greater than $\varepsilon_{\theta io}$ easily. Obviously, the outer pipe cannot recover its initial shape along the path (7→6) so that the residual internal stress P^* (or bonding stress) was produced in outer pipe's inner wall and equal and opposite external pressure is produced in inner pipe's outer wall. The stress path of inner pipe's outer wall is 3→4→5 and the stress path of outer pipe's inner wall is 7→8 because the deformation between inner pipe and outer pipe should coordinate each other. The radial and circumferential stress of outer pipe' inner wall is $\sigma^*_{\theta oi}$ and σ^*_{roi}, respectively, and the circumferential strain is $\varepsilon^*_{\theta oi}$ as shown at point 8. The new elastic deformation of inner pipe occurs and the stress ($\sigma^*_{\theta io}$ σ^*_{rio}) and the circumferential strain are produced due to the residual stress (P^*).

Where $\varepsilon^*_{\theta io}$ is negative. Tensile stress is positive and compressive stress is negative in this paper.

So the deformation compatibility condition (as Eq. (1)) of BP can be obtained according to the above analysis and Fig. 1

$$\varepsilon_{\theta io} + |\varepsilon^*_{\theta io}| = \varepsilon_{\theta oi} - \varepsilon^*_{\theta oi} \tag{1}$$

where $\varepsilon_{\theta io}$ is the recovered circumferential strain of inner pipe's outer wall when forming pressure was unloaded; $\varepsilon^*_{\theta io}$ (the circumferential strain of inner pipe's outer wall) is produced under the action of residual stress P^* (bonding stress); $\varepsilon_{\theta oi}$ is the recovered circumferential strain of outer pipe's inner wall when forming pressure was unloaded; and $\varepsilon^*_{\theta oi}$ (the circumferential strain of inner pipe's outer wall) is produced because of residual stress P^* (bonding stress) in the forming process.

According to Fig. 1, the total plastic strain of inner pipe can be obtained

$$\varepsilon^{**}_{\theta io} = |\varepsilon_{\theta i\Delta}| + |\varepsilon^*_{\theta oi}| + |\varepsilon^*_{\theta io}| \tag{2}$$

where $\varepsilon^{**}_{\theta io}$ is the total plastic strain of inner pipe' outer wall in forming process and $\varepsilon_{\theta i\Delta}$ is the circumferential strain of inner pipe' outer wall when the clearance between the inner pipe and outer pipe is eliminated.

2.2 The Elastic–Plastic Mechanical Analysis of Hydraulic Forming for BP. The outer pipe of BP is usually seamless steel tube, straight weld tube or spiral weld pipe, such as steel pipe, oil pipe and oil pipeline, etc., whose material is commonly carbon steel. Seamless pipe has initial ovality and eccentricity but straight weld pipe and spiral weld steel tube only have ovality. In addition, some residual stress will be produced for all of them in the production process. However, those factors are difficult to be considered in the theoretical model which can be used for calculation of the forming pressure. So in order to analyze the problem conveniently, the following hypotheses are made in this paper:

(1) The inner pipe and outer pipe have uniform thickness and they are the ideal cylinder.
(2) The mechanical properties of weld seams and pipe body are the same.
(3) The axial force is equal to zero in the forming process of BP.

The forming process of BP is considered as an axisymmetric plane stress problem based on the above mentioned hypotheses.

(1) The elastic analysis of cylindrical wall

Derived in Appendix A, the stress components $(\sigma_r, \sigma_\theta)$ under internal and external pressure can be described by

$$\begin{cases} \sigma_r = \dfrac{a^2b^2(P_b - P_a)}{b^2 - a^2}\dfrac{1}{r^2} + \dfrac{a^2P_a - b^2P_b}{b^2 - a^2} \\ \sigma_\theta = -\dfrac{a^2b^2(P_b - P_a)}{b^2 - a^2}\dfrac{1}{r} + \dfrac{a^2P_a - b^2P_b}{b^2 - a^2} \end{cases} \tag{3}$$

It is obvious that Eq. (3) has nothing to do with the elastic constants. So Eq. (3) is suitable for the plane stress problem and plane strain problem.

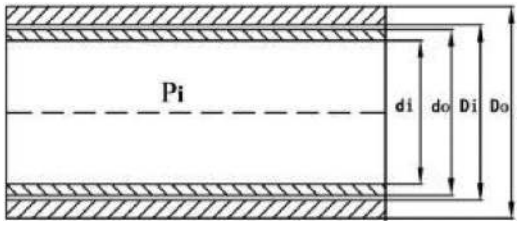

Fig. 2 Assembly structure of the BP

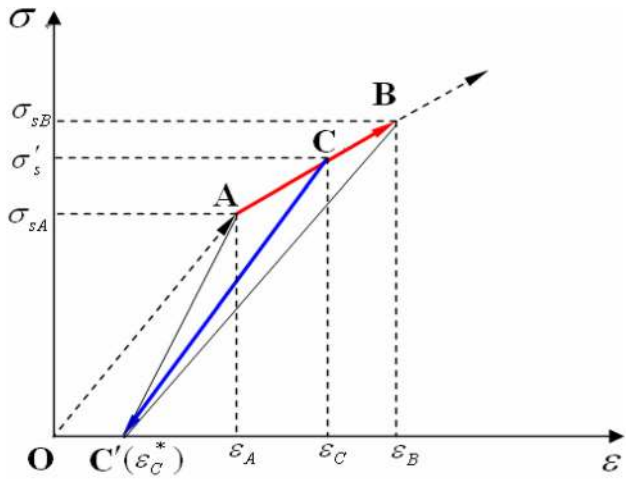

Fig. 3 Linear interpolation based on the linear hardening model in stress strain curve

where b is the external diameter of cylinder, mm; a is the internal diameter, mm; P_b is the external pressure of cylinder, MPa; P_a is the internal pressure, MPa; μ is the Poison's ratio of material; and E is the elastic modulus of material, MPa.

(2) The yield condition

The yield condition between the stress components $(\sigma_r, \sigma_\theta)$ must be satisfied when the material yields. Tresca yield criterion has been adopted in this paper as follows:

$$\sigma_\theta - \sigma_r = \sigma_s \tag{4}$$

2.3 The Stress Strain Analysis of the Inner and Outer Pipe in Hydraulic Forming Process. The assembly structure of the BP is as shown in Fig. 2. In Fig. 2, P_i is the forming pressure, (MPa); d_i is the inner diameter of inner pipe, (mm); d_o is the outer diameter of inner pipe, (mm); D_i is the inner diameter of outer pipe, (mm); and D_o is the outer diameter of outer pipe, (mm).

From Fig. 2, it is known that hydraulic forming process of BP should have three stages.

First stage: the clearance (Δ) between the inner and outer pipe is eliminated with the increase of forming pressure P_i, and there is no pressure acting on the outer pipe in this stage.

Second stage: The forming pressure goes on increasing after the clearance between the inner and outer pipe is eliminated and then the inner and outer pipes deform at the same time. And the inner pipe's inner wall is subjected to the internal pressure P_i and the outer wall is subjected to the external pressure P_C, while the outer pipe's inner wall is subject to the internal pressure P_C. The inner pipe is further strengthened because large plastic deformation is produced during this stage. But only the elastic deformation of outer pipe is produced during this stage.

Third stage: the pressure is unloaded in the inner and outer pipe at the same time; the outer pipe recovers along the original path (7→8 as shown in Fig. 1) and the inner pipe recovers linearly (along the path: 3→4 as shown in Fig. 1). After the pressure is unloaded, the residual stress P^* acts on the outer pipe's inner wall and an equal pressure P^* acts on the inner pipe's outer wall in the opposite direction.

The detailed analysis about the stress and strain of inner and outer pipe in the three stages is shown in Appendix B.

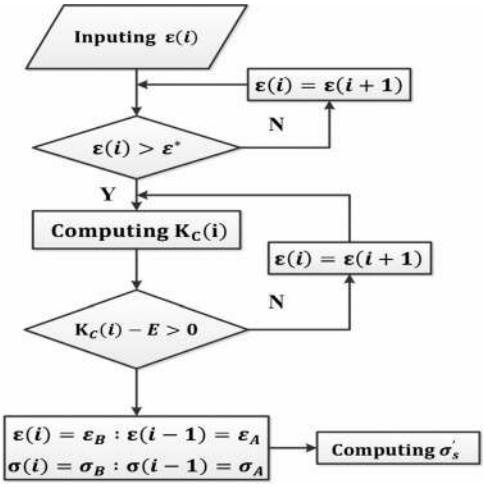

Fig. 4 The flow chart to calculate the plastic hardening stress

2.4 The Computing Method of Plastic Hardening Stress Based on the Stress Stain Curve. After getting the stress strain curve of the inner pipe, the plastic hardening stress can be obtained accurately by interpolation method between the adjacent measure points based on the linear hardening model. Thus, the computational accuracy of the plastic hardening stress depends on the density and the measurement accuracy of the data. If the point C is the maximum in the plastic deformation point of inner pipe, then the plastic strain of point C is ε_C^* and the stress of point C is ε_C^*. Points A and B nearest to the point C can always be found in the stress strain curve, as shown in Fig. 3.

In Fig. 3, point A corresponds to the point (stress: σ_{sA} and strain: ε_B); point B corresponds to the point (stress: $\varepsilon_s B$ and strain: ε_B); point C corresponds to the point (stress: 0, and strain: ε_C^*). According to the characteristic of linear rebound of inner pipe, the slope of the line CC' is equal to the elastic modulus of the inner pipe. The slope of the line AC'can be obtained by the stress and strain of point A and point C'. The slope of the line BC' can be obtained by the stress and strain of point B and point C'. Similarly, in the stress strain curve, the slope of the line C_iC' (recorded as k_c) can also be obtained. It is obvious that only the slope of the line AC' and the line BC' are the closest to the elastic modulus of the material.

In Fig. 3, the equation of the line CC' can be obtained according to the elastic modulus and the stress and strain of point C'. The equation of the line AB can be achieved by the stress and strain of the points A and B. Then, the stress and strain of the point C which is the intersection of the line CC' and the line AB can be considered according to the line CC' and the line AB. The plastic reinforcement stress of the point C can be obtained as follows:

$$\sigma_s' = \frac{\sigma_{sB} + \dfrac{\sigma_B - \sigma_A}{\varepsilon_B - \varepsilon_A}(\varepsilon_c^* - \varepsilon_B)}{1 - \dfrac{\sigma_B - \sigma_A}{(\varepsilon_B - \varepsilon_A)E_l}} \tag{5}$$

The flow chart which can calculate plastic hardening stress according to the stress and strain of measure points, as shown in Fig. 4.

2.5 The Calculation of Forming Pressure of BP in the Process of Hydraulic Forming. It is very critical to determine the size of forming pressure of BP in the process of hydraulic

forming because only the reasonable forming pressure can make the anticipated forming effect (high bonding strength or bonding stress P^* between internal and external pipe) achieved.

After unloading, total strain of outer wall of inner pipe is $(\varepsilon_{\theta io} - \varepsilon^*_{\theta io})$, the total strain can be obtained by Eqs. (B13) and (B20) as follows:

$$\varepsilon_{\theta io} - \varepsilon^*_{\theta io} = \frac{1}{E_i}\left[(\mu_i - 1)P_c + 2\sigma'_{si}\frac{\ln k}{k^z - 1}\right] + \frac{1}{E_i}\left[\frac{k^2+1}{k^2-1} - \mu_i\right]P^* \tag{6}$$

After unloading, total strain of outer pipe is $(\varepsilon_{\theta oi} - \varepsilon^*_{\theta oi})$, the total strain can be obtained by Eqs. (B16) and (B23) as follows:

$$\varepsilon_{\theta oi} - \varepsilon^*_{\theta oi} = \frac{1}{E_o}\left[\frac{k^2+1}{k^2-1} + \mu_o\right]P_C - \frac{1}{E_o}\left[\frac{k^2+1}{k^2-1} + \mu_o\right]P^* \tag{7}$$

By Eqs. (1), (B9), (6), and (7), Eq. (8) can be obtained

$$\frac{2\sigma'_{si}}{E_i}\frac{\ln k}{k^2-1} + \left\{\frac{1}{E_i}\left[\frac{k^2+1}{k^2-1} - \mu_i\right] + \frac{1}{E_o}\left[\frac{K^2+1}{K^2-1} + \mu_o\right]\right\}P^* = \left\{\frac{1}{E_i}(1-\mu_i) + \frac{1}{E_o}\left[\frac{K^2+1}{K^2-1} + \mu_o\right]\right\}(P_i - \sigma'_{si}\ln k) \tag{8}$$

where

$$A = \frac{2\sigma'_{si}}{E_i}\frac{\ln k}{k^2-1} \tag{9}$$

$$B = \frac{1}{E_i}(1-\mu_i) + \frac{1}{E_o}\left[\frac{K^2+1}{K^2-1} + \mu_o\right] \tag{10}$$

$$C = \frac{1}{E_i}\left[\frac{k^2+1}{k^2-1} - \mu_i\right] + \frac{1}{E_o}\left[\frac{K^2+1}{K^2-1} + \mu_o\right] \tag{11}$$

$$D = \sigma'_{si}\ln k \tag{12}$$

By Eqs. (8)–(12), Eq. (13) used for computing the forming pressure can be obtained

$$P_i = \frac{A}{B} + \frac{C}{D}P^* + D \tag{13}$$

Equations (8)–(13) was derived based on the plane stress condition. When the forming process of BP accords with the plane strain condition, constitutive equations under the plane stress condition need to be replaced by constitutive equations under the plane strain condition. The formula which is used for computing the forming pressure can be obtained.

Especially, when the elastic modulus and Poisson's ratio of the inside and outside of the tube is very close$(E_i = E_o, \mu_i = \mu_o)$, by Eq. (8), the following equation can be obtained:

$$P_i = \left[\frac{K^2-1}{2K^2} + \ln k\right]\sigma'_{si} + \frac{k^2K^2+1}{K^2(k^2-1)}P^* \tag{14}$$

Equation (14) is suitable for plane stress and plane strain problem because forming pressure P_i is independent on the mechanical parameters of material in Eq. (14).

It was known that forming pressure P_i is related to the mechanical parameters(E_i, μ_i, E_o, μ_o), geometric parameters (k, K) of material, the plastic hardening stress σ'_{si} of inner pipe, and bonding stress P^* according to Eqs. (8)–(13). The size of forming pressure depends on the size of the plastic hardening stress σ'_{si} of inner pipe and bonding stress P^* for the specific BP. However, the bonding stress P^* can be given by the user or manufacturer. So it is the foundation of calculating the forming pressure accurately to compute the plastic hardening stress of inner pipe reasonably.

Fig. 5 static strain test instrument (YJ-22)

From the stress strain curve of CRA [34], it is known that between the plastic hardening stress and plastic strain has one-to-one corresponding correlation. The plastic hardening stress σ'_{si} can be obtained from the stress strain curve of CRA according to total plastic strain of inner pipe (CRA). The total plastic strain $\varepsilon^{**}_{\theta io}$ of inner pipe in forming process can be obtained by Eqs. (2), (B20), and (B23) when the bonding stress is known

$$\varepsilon^{**}_{\theta io} = \left|\frac{\Delta}{r_o}\right| + \left|\frac{1}{E_o}\left[\frac{K^2+1}{K^2-1} + \mu_o\right]P^*\right| + \left|\frac{1}{E_i}\left[\frac{k^2+1}{k^2-1} - \mu_i\right]P^*\right| \tag{15}$$

When the forming pressure is larger than the minimum forming pressure (the forming pressure which makes inner and outer pipe just joining together (bonding stress P^* is equal to zero) is the minimum forming pressure), the larger plastic strain of inner pipe would be produced and it can lead to further hardening of inner pipe. However, in Wang's work, when the clearance between the BP was eliminated, the yield stress $\sigma_{si\Delta}$ of inner pipe was used to compute the forming pressure [33]. So the consideration for plastic deformation of inner pipe is not enough. In addition, Wang's method is not practical because the hardening modulus is difficult to get for the forming pressure calculation.

By Eqs. (11) and (15), Eq. (16) can be given

$$\varepsilon^{**}_{\theta io} = \left|\frac{\Delta}{r_o}\right| + |CP^*| \tag{16}$$

The plastic hardening stress σ'_{si} (the computing method is obtained in Sec. 2.4) can be obtained according to Eq. (16) and the stress strain curve of inner pipe when the geometric parameters and mechanical parameters of BP and the bonding stress P^* are known. Then, the forming pressure can be directly obtained according to Eq. (13). However, the bonding stress cannot be obtained directly by Eq. (13) when the forming pressure is known. The bonding stress can be got only by iteration method because there are two unknowns in Eq. (13).

3 The Hydraulic Forming Test of BP and Strain Test in the Forming Process

3.1 Sample Preparation. The stainless steel pipe (63×0.76 mm) was chosen as the inner pipe of BP. Its mechanical parameters and the one-to-one corresponding relationship between the plastic hardening stress σ'_{si} and plastic strain $\sigma^*_{\theta oi}$ can be obtained from the literature [34]. The carbon steel (T95) pipe (70×3.5 mm) was chosen as the outer pipe of BP. Its elastic modulus E is equal to 206,000 MPa and its Poisson's ratio is equal to 0.3.

3.2 The Experiment Equipment

(1) A pressure test pump and its rated pressure was 60 MPa.
(2) A static strain test instrument (YJ-22) is shown as in Fig. 5.
(3) A sealing arrangement of hydraulic forming for BP is shown as in Fig. 6.

3.3 The Experimental Program of Hydraulic Forming for BP. The stainless steel pipe (63×0.76 mm) was chosen as the inner pipe of BP and the carbon steel pipe (70×3.5 mm) was

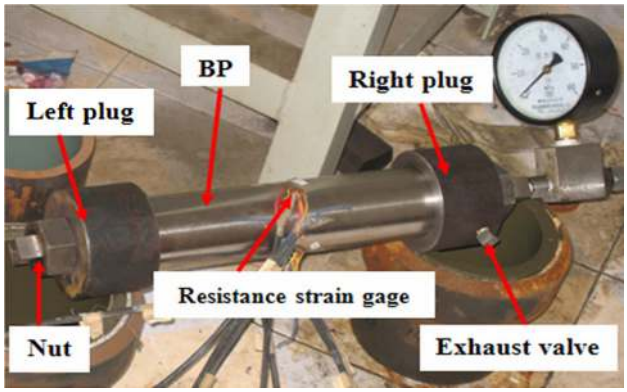

Fig. 6 The sealing arrangement of hydraulic forming for bimetal-pipe

chosen as the outer pipe of BP. The strain of outer pipe was measured in the loading and unloading process. The forming pressure P_i was measured and the residual strain of outer pipe was obtained in different forming pressure. The minimum forming pressure (28.18 MPa) can be obtained according to the theoretical model of this paper; however, the allowed maximum was 48 MPa considering the safety of hydraulic system. So the loading sequence of test was 0 MPa→26 MPa→0 MPa→31 MPa→0 MPa →42 MPa→0 MPa→48 MPa→0 MPa. The experimental program of hydraulic forming for BP and relevant parameters is shown in Table 1. In Table 1, E is elastic modulus of material and μ is Poison's ratio.

3.4 Test Results and Analysis of Hydraulic Forming. The surface appearance of BP is shown in Fig. 7 after hydraulic forming. From Fig. 7, it was known that the connection between the inner pipe and outer pipe is tight so that the clearance between the inner pipe and outer pipe was not seen by the naked eyes. The measured strain (the mean strain of many measured point) of outer pipe was as shown in Figs. 8–11 and Table 2. Figure 8 was circumferential strain-forming pressure relation curves of outer pipe, when the loading sequence of test was 0 MPa→26 MPa→0. Figure 9 was circumferential strain- forming pressure relation curves of outer pipe, when the loading sequence of test was 0 MPa→31 MPa→0. Figure 10 was circumferential strain-forming pressure relation curves of outer pipe, when the loading sequence of test was 0 MPa→42 MPa→0. Figure 11 was circumferential strain- forming pressure relation curves of outer pipe, when the loading sequence of test was 0 MPa→48 MPa→0.

From Fig. 8, it was known that the deformation of outer pipe did not take place at the beginning of loading until the forming pressure was larger than 4 MPa. It indicated that there was a gap between the inner and outer pipe. The result obtained was in agreement with the real size of inner and outer pipe as shown in Table 1. Residual strain of outer pipe was not produced in the process of unloading (from 26 MPa to 0 MPa). It indicated that the outside wall of inner pipe and the inside wall of outer pipe did not contact when the forming pressure is equal to 26 MPa. The result is in agreement with the minimum forming pressure 28.18 MPa (see Table 1) calculated by this theoretical model. The test and theoretical results indicate there is a critical forming pressure in

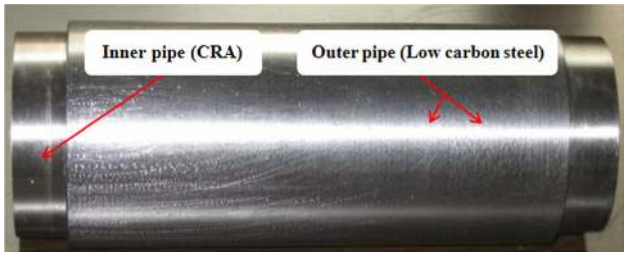

Fig. 7 The morphology of BP after hydraulic forming

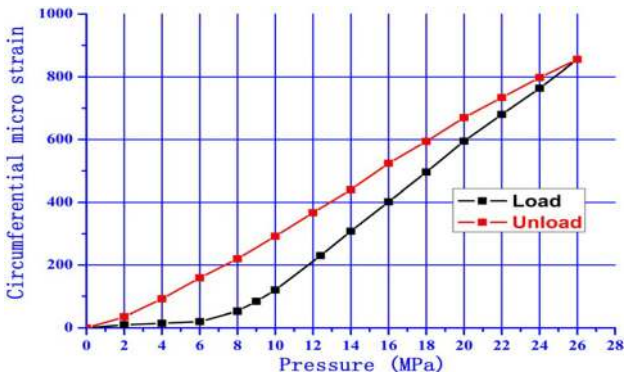

Fig. 8 Circumferential microstrain of outer pipe in the process of load and unload (0–26 MPa)

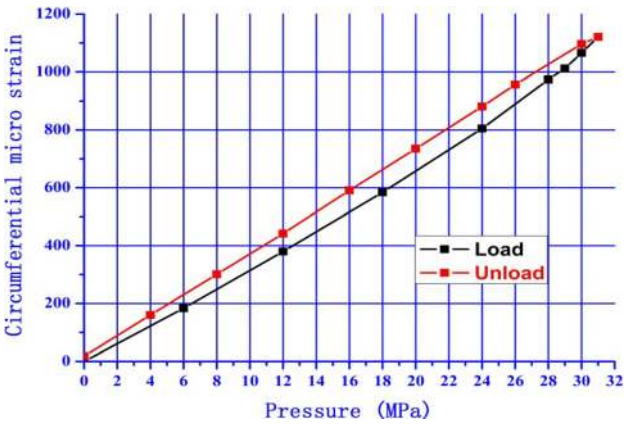

Fig. 9 Circumferential microstrain of outer pipe in the process of load and unload (0–31 MPa)

the forming process of BP. The forming pressure used to produce BP should be more than the critical forming pressure which is the key technique indicator of producing BP.

From Fig. 9, it was known that circumferential strain of outer pipe increased linearly before the forming pressure was equal to 24 MPa. After the forming pressure was equal to 28 MPa, circumferential strain of outer pipe increased faster obviously because inner pipe produced new plastic deformation. The recovery of

Table 1 Experiment program of hydraulic forming for BP and relevant parameters

	Geometric and mechanical parameters of outer pipe				Geometric and mechanical parameters of inner pipe				Forming pressure (MPa)		
BP	Outer diameter (mm)	Inner diameter (mm)	E GPa	μ	Outer diameter (mm)	Wall thickness (mm)	E (GPa)	μ	Min	Max	Forming method
Sample	70	63.02	206	0.3	63	0.76	188.9	0.3	28.18	48	Hydraulic

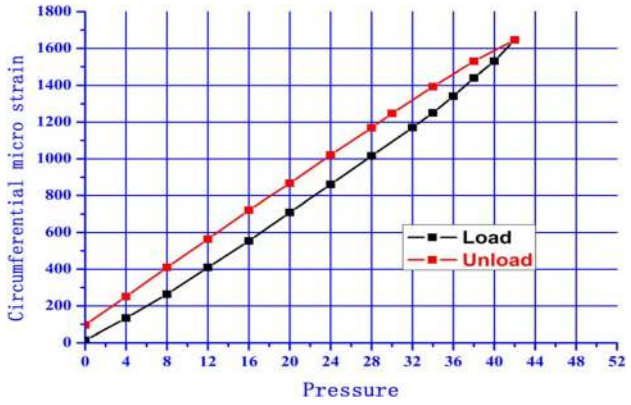

Fig. 10 Circumferential microstrain of outer pipe in the process of load and unload (0–42 MPa)

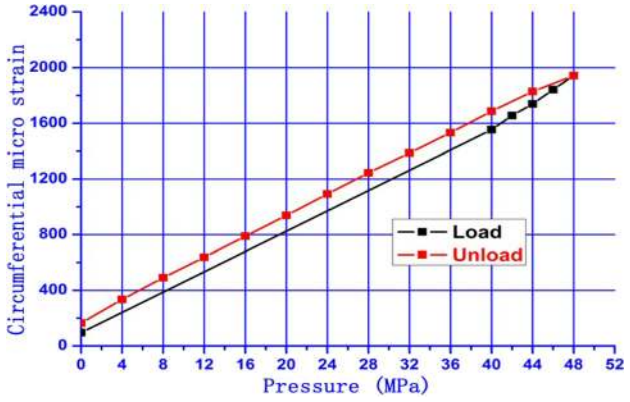

Fig. 11 Circumferential microstrain of outer pipe in the process of load and unload (0–48 MPa)

circumferential strain of outer pipe is linear and new residual strain was produced in the process of unloading (from 31 MPa to 0 MPa). The bonding stress P^* can be obtained by Eq. (B23). The residual strain $\varepsilon^*_{\theta io}$ of the outer wall of inner pipe can be obtained by Eq. (B20). The plastic hardening stress σ'_{si} can be obtained by Eq. (15) and the calculation method of this paper. Those computed results are shown in the Table 2.

From Fig. 10, it was known that circumferential strain of outer pipe increased linearly before the forming pressure was equal to 28 MPa. After the forming pressure was equal to 32 MPa, circumferential strain of outer pipe increased faster obviously because inner pipe produced new plastic deformation. The recovery of circumferential strain of outer pipe is linear and new residual strain was produced in the process of unloading. Similarly, bonding stress P^* and the residual strain $\varepsilon^*_{\theta io}$ of the outer wall of inner pipe and the plastic hardening stress σ'_{si} can be obtained (see Table 2).

From Fig. 11, it was known that circumferential strain curve of outer pipe increased faster after forming pressure was equal to 42 MPa. The recovery of circumferential strain of outer pipe is linear and new residual strain was produced in the process of unloading. Similarly, bonding stress P^* and the residual strain $\varepsilon^*_{\theta io}$ of the outer wall of inner pipe and the plastic hardening stress σ'_{si} can be obtained (see Table 2).

The experimental data in Table 2 were plotted into curves as shown in Fig. 12 for discussing the relationship between forming pressure and test results (residual strain of outer pipe, bonding stress, total plastic strain and plastic hardening stress of inner pipe). The test results have a linear relation with the forming pressure. The test results increase with the increase of forming pressure. So, the bonding stress which is one of the key performance

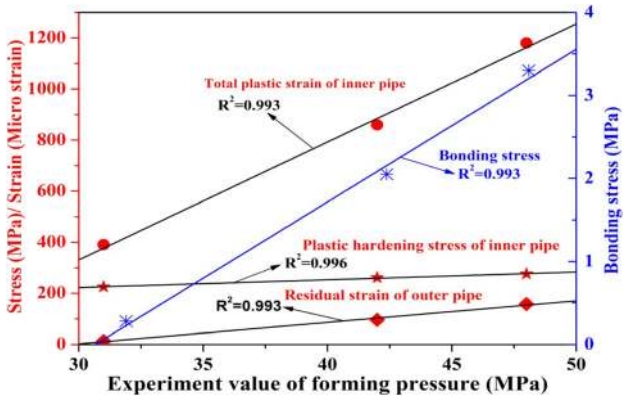

Fig. 12 The relationship between forming pressure and test results

indicators of BP [35] can be very well controlled by the forming pressure.

4 Theoretical and Experimental Comparisons

In order to validate the correctness of this theoretical model and method, the geometric parameters and mechanical parameters of inner and outer pipe in the Table 1 and bonging pressure P^* and the plastic hardening stress σ'_{si} of inner pipe in Table 2 were plugged into Eqs. (9)–(13).The forming pressure P_i can be obtained by computing those equations and the results were shown in Table 3. From Table 3, it was known that the calculating

Table 2 Stress and strain of inner and outer pipe under forming pressure

Experiment value of forming pressure (MPa)	Residual strain of outer pipe ($\times 10^{-6}$)	Bonding stress P^* (MPa)	Total plastic strain of inner pipe $\varepsilon^{**}_{\theta io}$ ($\times 10^{-6}$)	the plastic hardening stress of inner pipe σ'_{si} (MPa)
31	13.33	0.28	390.74	225
42	96	2.01	845.85	261
48	158	3.30	1187.17	276

Table 3 Contrast of experimental value with the theoretical value of forming pressure

			Theoretical model of this paper	
Experiment value of forming pressure (MPa)	Bonding stress P^* (MPa)	The plastic hardening stress of inner pipe σ'_{si} (MPa)	The calculated value of forming pressure: P_i (MPa)	Error (%)
31	0.28	226	29.65	4.35
42	2.01	261	42.73	1.74
48	3.30	276	50.86	5.96

errors are all under 6%. Thus, in the range of error which can be accepted by engineering, the calculation result is in agreement with the experimental result.

5 Conclusions

(1) Based on the stress strain curve and hardening characteristics of material, the stress strain characteristics curve and the correlation between stress and strain of BP in the forming process have been plotted, so that the deformation compatibility condition of BP in hydraulic forming process has been obtained.
(2) According to the law of plastic deformation in the forming process of BP, the method which is used for computing the plastic hardening stress has been proposed based on the stress and strain curve of inner pipe.
(3) Based on the nonlinear kinematic hardening characteristics of material the mechanical model which is used for computing the forming pressure in the forming process of BP has been established; the accurate computing method has been obtained according to the method of computing the plastic hardening stress and the deformation compatibility condition of BP.
(4) The experimental study of hydraulic forming process for BP has been performed and experimental results are consistent with results of calculation of model. It indicates that the model can be used to provide theoretical guidance for the design and production as well as use of BP.

Acknowledgment

Research work was cofinanced by the National Natural Science Foundation of China (Nos. 51274170 and 51004084). Without their support, this work would not have been possible.

Appendix A: Elastic Analysis of Cylindrical Wall

According to the theory of elastic–plastic mechanics, the balance equation (A1) of plane axisymmetric problem can be obtained

$$\frac{d\sigma_r}{dr}+\frac{\sigma_r-\sigma_\theta}{r}=0 \tag{A1}$$

And the geometric equation (A2) also can be obtained

$$\begin{cases}\varepsilon_r=\dfrac{du}{dr}\\ \varepsilon_\theta=\dfrac{u}{r}\end{cases} \tag{A2}$$

And the constitutive equation (A3) also can be obtained

$$\begin{cases}\varepsilon_r=\dfrac{1}{E}(\sigma_R-\mu\sigma_\theta)\\ \varepsilon_\theta=\dfrac{1}{E}(\sigma_\theta-\mu\sigma_r)\\ \varepsilon_z=\dfrac{\mu}{E}(\sigma_\theta+\sigma_R)\end{cases} \tag{A3}$$

By Eq. (A2), the deformation compatibility equation (A4) can be obtained

$$\frac{\mathrm{d}\varepsilon_\theta}{\mathrm{dr}}+\frac{\varepsilon_\theta-\sigma_\mathrm{r}}{\mathrm{r}}=0 \tag{A4}$$

By Eqs. (A3) and (A4), Eq. (A5) which is expressed as the stress can be obtained

$$\frac{d\sigma_\theta}{dr}-\mu\frac{d\sigma_r}{dr}=\frac{1+\mu}{r}(\sigma_r-\sigma_\theta) \tag{A5}$$

By Eq. (A1), Eq. (A6) can be obtained

$$\sigma_\theta=\sigma_r+r\frac{d\sigma_r}{dr} \tag{A6}$$

By taking a derivative with respect to r in Eq. (A6), Eq. (A7) can be obtained

$$\frac{d\sigma_\theta}{dr}=r\frac{d^2\sigma_r}{dr^2}+2\frac{d\sigma_r}{dr} \tag{A7}$$

By Eqs. (A5)–(A7), Eq. (A8) can be obtained

$$\frac{d^2\sigma_r}{dr^2}+\frac{3}{r}\frac{d\sigma_r}{dr}=0 \tag{A8}$$

Equation (A8) can be simplified as Eq. (A9)

$$\frac{d(\sigma_r')}{\sigma_r'}=-3\frac{dr}{r} \tag{A9}$$

Equation (A10) can be obtained by integrating Eq. (A9)

$$\sigma_r=-\frac{C}{2r^2}+C_1=C_1+\frac{C_2}{r^2} \tag{A10}$$

By Eqs. (3), (10), and (11) can be obtained

$$\sigma_\theta=C_1-\frac{C_2}{r^2} \tag{A11}$$

When the uniform internal pressure on the inner wall is equal to P_a and the uniform external pressure on the outer wall is equal to P_b, the boundary conditions of inner and outer wall can be given as follows:

$$\begin{cases}(\sigma_r)_{r=b}=P_b\\ (\sigma_r)_{r=a}=P_a\end{cases} \tag{A12}$$

By Eqs. (A10) and (A12), Eq. (A13) can be obtained

$$\begin{cases}C_1=\dfrac{1}{b^2-a^2}(a^2P_a-b^2P_b)\\ C_2=\dfrac{a^2b^2}{b^2-a^2}(P_b-P_a)\end{cases} \tag{A13}$$

By Eqs. (A10), (A11), and (A13), the stress components (σ_r,σ_θ) can be obtained

$$\begin{cases}\sigma_r=\dfrac{a^2b^2(P_b-P_a)}{b^2-a^2}\dfrac{1}{r^2}+\dfrac{a^2P_a-b^2P_b}{b^2-a^2}\\ \sigma_\theta=-\dfrac{a^2b^2(P_b-P_a)}{b^2-a^2}\dfrac{1}{r}+\dfrac{a^2P_a-b^2P_b}{b^2-a^2}\end{cases} \tag{A14}$$

Appendix B: Analysis of Stress and Strain

(1) Analysis of stress and strain in the first stage

There is no pressure acting on the outer pipe in the first stage. The inner pipe is subjected to the forming pressure P_i and the circumferential stress σ_θ and radial stress σ_r can be obtained by Eq. (A14)

$$\begin{cases}\sigma_r=\dfrac{P_l}{k^2-1}\left[1-\dfrac{r_\mathrm{o}^2}{r^2}\right]\\ \sigma_\theta=\dfrac{P_l}{k^2-1}\left[1+\dfrac{r_\mathrm{o}^2}{r^2}\right]\end{cases} \tag{B1}$$

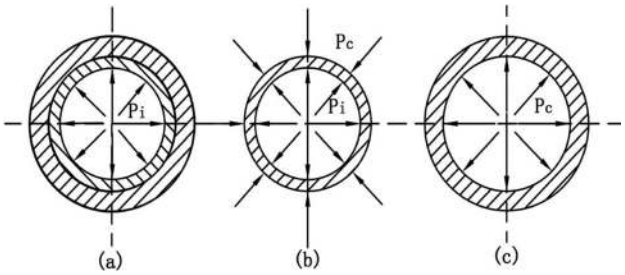

Fig. 13 The force diagram during the forming stage of BP: (*a*) assembly of the BP; (*b*) inner pipe, and (*c*) outer pipe)

where P_i is forming pressure, MPa; r is the inside radius of inner pipe, mm; and r_o is the outer radius of inner pipe, mm; k ((d_o/d_i) or (r_o/r_i)) is the ratio of outer radius and the inside radius of inner pipe.

By Eq. (B1) and Tresca yield criterion, the forming pressure or elastic limiting pressure P_{iie} which makes the inner pipe's inner wall just yield can be obtained

$$P_{iie} = \frac{\sigma_{si}(k^2-1)}{2k^2} \tag{B2}$$

where σ_{si} is the yield strength of inner pipe, MPa. (The yield strength is not $\sigma_{0.2}$ and it is the stress making the inner pipe's inner wall just begin yield.)

The plastic zone of inner pipe expands from inside to outside when the forming pressure is greater than elastic limiting pressure P_{iie}. Hence, larger plastic deformation is produced.

By Eq. (A1) and Tresca yield criterion, Eq. (B3) can be obtained

$$\frac{d\sigma_r}{dr} - \frac{\sigma_s}{r} = 0 \tag{B3}$$

By solving Eq. (B3), Eq. (B4) can be obtained

$$\sigma_r = \sigma_s \ln r + C \tag{B4}$$

where C is integration constant; C $(C = -P_i - \sigma_s \ln r_i)$ can be obtained by Eq. (B4) according to the boundary condition $(\sigma_r|r = r_i = -P_i)$. The circumferential stress σ_θ can be obtained according to Tresca yield criterion. When inner pipe yielded completely, the circumferential stress σ_θ and radial stress σ_r was as follows:

$$\begin{cases} \sigma_r = \sigma_{si} \ln \frac{r}{r_l} - P_i \\ \sigma_\theta = \sigma_{si}\left(1 + \ln \frac{r}{r_l}\right) - P_i \end{cases} \tag{B5}$$

The forming pressure which makes inner pipe completely yield can be obtained by Eq. (B5) according to the boundary condition $(\sigma_r|r = r_o = 0)$

$$P_{iip} = \sigma_{si} \ln k \tag{B6}$$

By Eqs. (A2), (A3), (B5), (B6) and Tresca yield criterion, when the inner pipe yields completely the radial displacement of inner pipe's outer wall can be obtained

$$u_{iop} = \frac{\sigma_{si}}{Ei} r_o \tag{B7}$$

In order to assemble the inner pipe and out pipe easily, the gap (clearance) between the inner and outer pipe is large enough due to the ovality and eccentricity of pipe. The radial displacement u_{iop} is less than the gap Δ between the inner pipe and outer pipe, when the inner pipe yields completely. Thus, for the purpose of achieving large deformation of the inner pipe the forming pressure needs to be increased. After forming pressure is greater than the pressure which makes the inner pipe yield completely, the larger plastic deformation is produced and the material is strengthened. The wall thickness of inner pipe is considered to be the same in the forming process, because the expansion of inner pipe is very small (because of small clearance Δ) under the action of internal pressure. When the gap between the inner pipe and outer pipe is eliminated the forming pressure can be obtained

$$P_i = \sigma_{si\Delta} \ln k \tag{B8}$$

where $\sigma_{si\Delta}$ is the plastic hardening stress, when the gap between the inner pipe and outer pipe is eliminated, MPa.

(2) Analysis of stress and strain in the second stage

The forming pressure continues increasing after the gap Δ between the inner pipe and outer pipe is eliminated. At that moment, the deformation of inner pipe and outer pipe occurs simultaneously and the internal pressure which the inner pipe's inner wall is subjected to is equal to P_i; the external pressure which the inner pipe's outer wall is subjected to is equal to P_c; the internal pressure which the outer pipe's inner wall is subjected to is equal to P_c, as shown in Fig. 13. When the forming pressure is unloaded, P_c will exists for ever, which is called bonding stress.

Where Fig. 13(*a*) is the force diagram of BP; Fig. 13(*b*) is the force diagram of the inner pipe of BP; Fig. 13(*c*) is the force diagram of the outer pipe of BP.

By Eq. (B5), the forming pressure can be obtained according to the boundary condition $(\sigma_r|r = r_o = -P_c)$

$$P_i = P_c + \sigma'_{si} \ln k \tag{B9}$$

where σ'_{si} is the plastic hardening stress of inner pipe under the forming pressure (P_i).

When the forming pressure is unloaded the stress and strain of inner and outer pipe is eliminated obeying the elastic law. By Eq. (A14), the eliminated stress can be obtained

$$\begin{cases} \bar{\sigma}_r = \frac{P_l}{k^2-1}\left[1 - \frac{r_o^2}{r^2}\right] - \frac{P_c k^2}{k^2-1}\left[1 - \frac{r_i^2}{r^2}\right] \\ \bar{\sigma}_\theta = \frac{P_l}{k^2-1}\left[1 + \frac{r_o^2}{r^2}\right] - \frac{P_c k^2}{k^2-1}\left[1 + \frac{r_i^2}{r^2}\right] \end{cases} \tag{B10}$$

By Eq. (B10), the eliminated stress of inner pipe's outer wall $(r = r_o)$ can be obtained

$$\begin{cases} \bar{\sigma}_{rio} = -P_c \\ \bar{\sigma}_{\theta io} = -P_c + 2\sigma'_{si}\frac{\ln k}{k^2-1} \end{cases} \tag{B11}$$

where $\bar{\sigma}_{\theta io}$ is the eliminated circumferential stress of inner pipe's outer wall and $\bar{\sigma}_{rio}$ is eliminated radial stress of inner pipe's outer wall, MPa.

By Eq. (A3), the eliminated strain of inner pipe's outer pipe can be obtained

$$\varepsilon_{\theta io} = \frac{1}{E_i}(\bar{\sigma}_{\theta io} - \mu_i \bar{\sigma}_{rio}) \tag{B12}$$

By Eqs. (B11) and (B12), Eq. (B13) can be obtained

$$\varepsilon_{\theta io} = \frac{1}{E_i}\left[(\mu_i - 1)P_c + 2\sigma'_{si}\frac{\ln k}{k^2-1}\right] \tag{B13}$$

By Eq. (A14), the eliminated stress of outer pipe can be obtained according to Fig. 3

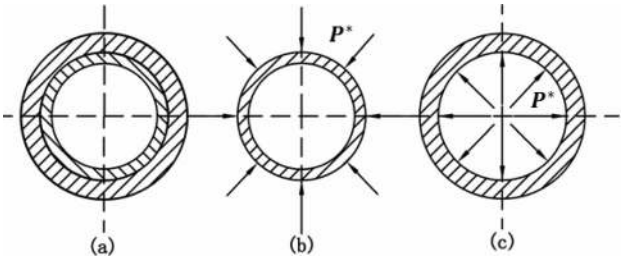

Fig. 14 The force diagram of formed BP: (*a*) assembly of the BP; (*b*) inner pipe, and (*c*) outer pipe)

$$\begin{cases} \sigma_r = \frac{P_c}{K^2-1}\left[1-\frac{R_o^2}{R^2}\right] \\ \sigma_\theta = \frac{P_c}{K^2-1}\left[1+\frac{R_o^2}{R^2}\right] \end{cases} \tag{B14}$$

where P_c is the internal pressure acting on the outer pipe, MPa; R_i is the inside radius of outer pipe, mm; $R_o$is the outside radius of outer pipe, mm; and K ($\boldsymbol{D_o/D_i}$ or $\boldsymbol{R_o/R_i}$) is the ratio of R_o and R_i.

By Eq. (B14), the alternative stress of outer pipe's inner wall can be obtained (where $R = R_i$)

$$\begin{cases} \bar{\sigma}_{roi} = -P_c \\ \bar{\sigma}_{\theta oi} = \dfrac{K^2+1}{K^2-1}P_c \end{cases} \tag{B15}$$

where $\bar{\sigma}_{roi}$ is the eliminated circumferential stress of outer pipe's inner wall and $\bar{\sigma}_{\theta oi}$ is eliminated radial stress of outer pipe's inner wall, MPa.

Similarly, the alternative strain of outer pipe's inner wall because of the unloading of the forming pressure can be obtained, by Eqs. (A3) and (B15)

$$\varepsilon_{\theta oi} = \frac{1}{E_o}\left[\frac{K^2+1}{K^2-1}-\mu_o\right]P_C \tag{B16}$$

where $\boldsymbol{E_O}$ is the elastic modulus of outer pipe, MPa and μ_o is the Poisson's ratio of outer pipe.

(3) Analysis of stress and strain in the third stage

After the forming pressure P_i is unloaded, the internal pressure which the outer pipe's inner wall is subjected to is equal to the bonding stress (P^*); the external pressure which the inner pipe's outer wall is subjected to is equal to bonding stress (P^*), as shown in Fig. 14.

Where Fig. 14(*a*) is the diagram of BP; Fig. 14(*b*) is the force diagram of inner pipe; Fig. 14(*c*) is the diagram of outer pipe.

By Eq. (A14), the stress components of inner pipe can be obtained under the action of external pressure (P^*)

$$\begin{cases} \sigma_r^* = \dfrac{P^*k^2}{K^2-1}\left[1-\dfrac{r_i^2}{r^2}\right] \\ \sigma_\theta^* = \dfrac{P^*}{K^2-1}\left[1+\dfrac{r_I^2}{r^2}\right] \end{cases} \tag{B17}$$

By Eq. (B17), the stress of inner pipe's outer wall can be obtained (when $r = r_o$)

$$\begin{cases} \sigma_{rio}^* = -P^* \\ \sigma_{\theta io}^* = -\dfrac{K^2+1}{K^2-1}P^* \end{cases} \tag{B18}$$

where $\sigma_{\theta io}^*$ is the circumferential stress of inner pipe's outer wall, MPa and σ_{rio}^* is the radial stress of inner pipe's outer wall, MPa.

By Eq. (A3), the produced strain of inner pipe's outer wall can be obtained under the action of external pressure (P^*)

$$\varepsilon_{\theta io}^* = -\frac{1}{E_i}(\sigma_{\theta io}^* - \mu\sigma_{rio}^*) \tag{B19}$$

By Eqs. (B18) and (B19), Eq. (B20) can be obtained

$$\varepsilon_{\theta io}^* = -\frac{1}{E_i}\left[\frac{K^2+1}{K^2-1}-\mu_i\right]P^* \tag{B20}$$

By Eq. (A14), the stress components of outer pipe can be obtained under the action of internal pressure (bonding stress P^*)

$$\begin{cases} \sigma_r = \dfrac{P^*}{K^2-1}\left[1-\dfrac{R_o^2}{R^2}\right] \\ \sigma_\theta = \frac{P^*}{K^2-1}\left[1+\dfrac{R_o^2}{R^2}\right] \end{cases} \tag{B21}$$

By Eq. (B21), the stress of out pipe's inner wall can be obtained (when $R = R_i$)

$$\begin{cases} \sigma_{roi}^* = -P^* \\ \sigma_{\theta oi}^* = \dfrac{K^2+1}{K^2-1}P^* \end{cases} \tag{B22}$$

where $\sigma_{\theta oi}^*$ is the circumferential stress of outer pipe's inner wall, MPa and σ_{roi}^* is the radial stress of outer pipe's inner wall, MPa.

Similarly, by Eqs. (A3) and (B23), the strain of outer pipe's inner wall can be obtained under the action of internal pressure (P^*)

$$\varepsilon_{\theta oi}^* = \frac{1}{E_o}\left[\frac{K^2+1}{K^2-1}+\mu_o\right]P^* \tag{B23}$$

References

[1] Eckert, R. B., Bensman, L. A., and Weichel, S. J., 2012, "Employing Forensic Corrosion Engineering in a Corrosion Management System," NACE International, L. A. Bensman et al., eds., Paper No. 2012-1636.

[2] Fei, C., and Yi, R. W., 2005, "Mechanism of CO2 Corrosion in High Pressure and Condensate Gas Wells and Techniques for Preventing It," J. Oil Gas Technol., **27**(1), pp. 297–299.

[3] Wei, L. X., Min, G. Y., 2009, "Present Situation and Protection Methods of CO2 Corrosion," Corros. Sci. Prot. Technol., **21**(6), pp. 553–555.

[4] Dezhi, Z., Qingsong, D., Tan, G., Liming, H., Zhi, Z., and Taihe, S., 2008, "The Research Progress in the Anti-Corrosion Technology of Bimetal Pipe," Oil-Gasfield Surf. Eng., **27**(12), pp. 64–65.

[5] Kroon, D. H., Lindemuth, D. D., Sampson, S. L., and Vincenzo, T., 2004, "Corrosion Protection of Ductile Iron Pipe," NACE International, Paper No. 04046.

[6] Ahmad, I., Gazwi, R. H., and Elosheby, I. I. M., 2011, "Pipeline Integrity Management Through Corrosion Mitigation and Inspection Strategy in Corrosive Environment: An Experience of Arabian Gulf Oil Company in Libya," NACE International, Paper No. 11311.

[7] NACE International, 2012, "Measurement Techniques Related to Criteria for Cathodic Protection on Underground or Submerged Metallic Piping Systems," NACE International, Paper No. TM0479-2012.

[8] Aberle, D., and Agarwal, D. C., 2008, "High Performance Corrosion Resistant Stainless Steels and Nickel Alloys for Oil & Gas Applications," NACE International, Paper No. 08085.

[9] Shukla, C. P. K., Pabalan, R., and Yang, L., 2010, "On Development of Accelerated Testing Methods for Evaluating Organic Coating Performance Above 100 ° C," NACE International, Paper No. 10006.

[10] Shouse, L., Logan, M., Brock, G., and McCormic, H. G., 2012, "Corrosion Prevention Technology Break-Through," NACE International, Paper No. 2012-1611.

[11] Okunola, A., and Slogvik, B., 2012, "Cathodic Protection of a Land Pipeline With Fjord Crossings," NACE International, Paper No. 2012-1544.

[12] Jevremovic, I., Miskovic-Stankovic, V. B., Achour, M., Blumer, D., Baugh, T., Singer, M., and Nesic, S., 2012, "A Novel Method to Mitigate the Top of the Line Corrosion in Wet Gas Pipelines by Corrosion Inhibitor Within a Foam Matrix," NACE International, Paper No. 2012-1403.

[13] Arora, A., and Bareli, R., 2012, "Review on Materials for Corrosion Prevention in Oil Industry," Society of Petroleum Engineers, Paper No. 155211-MS.
[14] Lauer, R. S., 2012, "Existing and New Coating Technologies for Drilling and Completion Applications," Society of Petroleum Engineers, Paper No.152836-MS.
[15] Nikitina, L. A., 1998, "Status and Prospects for the Manufacture of Multilayered and Bimetallic Metal Products," Metallurgist, **42**(8), pp. 297–301.
[16] Rommerskirchen, I., 2005, "New Progress Caps 10 Years of Work With BuBi Pipes," World Oil, **226**(7), pp. 69–70.
[17] Focke, E. S., Gresnigt, A. M., Meek, J., and Nakasugi, H., 2004, "The 2-Dimensional Modelling of the Manufacturing Process of Tight Fit Pipe (TFP)," The International Society of Offshore and Polar Engineers, Paper No. I-04-146.
[18] Toguyeni, G. A., and Banse, J., 2012, "Mechanically Lined Pipe: Installation by Reel-Lay," Offshore Technology Conference, Paper No. 23096-MS.
[19] Denniel, S., Tkaczyk, T., and Smith, D., 2011, "Reelable Cost Effective and Enabling Pipeline Technologies," Offshore Technology Conference, Paper No. 21487-MS.
[20] Prohaska, M., Tischler, G., Mori, G., Grill, R., and Hofst, H., 2011, "Corrosion Properties of Different Highly Alloyed Clad Materials for Offshore Applications Manufactured by a New Thermo-Mechanical Rolling Process," NACE International, Paper No.11175.
[21] Burke, R. N., and Ody, T., 2010, "Intelligent Pipeline Design and Construction," Society of Petroleum Engineers, Paper No.127880-MS.
[22] Gomez, X., and Echeberria, J., 2003, "Microstructure and Mechanical Properties of Carbon Steel A2102 Superalloy Sanicro 28 Bimetallic Tubes," Mater. Sci. Eng., **348**(122), pp. 180–191.
[23] Haiyun, C., and Zhixi, C., 2006, "Application and Development of Plastic Forming Technique for Double Metal Combined Pipe," Process Equip. Piping, **43**(5), pp. 16–18.
[24] Torbati, A. M., Miranda, R. M., Quintino, L., and Williams, S., 2011, "Welding Bimetal Pipes in Duplex Stainless Steel," Int. J. Adv. Manuf. Technol., **53**(9–12), pp. 1039–1047.
[25] Chen, W.-C., and Petersen, C. W., 1992, "Corrosion Performance of Welded CRA-Lined Pipes for Flowlines," Society of Petroleum Engineers, Paper No.22501-PA.
[26] Watanabe, Y., Inaguma, Y., and Sato, H., 2011, "Cold Model for Process of a Ni-Aluminide/Steel Clad Pipe by a Reactive Centrifugal Casting Method," Mater. Lett., **65**(3), pp. 467–470.
[27] An, H., Green, D. E., and Johrendt, J., 2010, "Multi-Objective Optimization and Sensitivity Analysis of Tube Hydroforming," Int. J. Adv. Manuf. Technol., **50**(1–4), pp. 67–84.
[28] Hashemi, R., Faraji, G., Abrinia, K., and Dizaji, A. F., 2010, "Application of the Hydroforming Strain-and Stress-Limit Diagrams to Predict Necking in Metal Bellows Forming Process," Int. J. Adv. Manuf. Technol., **46**(4-8), pp. 551–561.
[29] Li, S., Xu, X., Zhang, W., and Lin, Z., 2009, "Study on the Crushing and Hydroforming Processes of Tubes in a Trapezoid-Sectional Die," Int. J. Adv. Manuf. Technol., **43**(1–2), pp. 67–77.
[30] Reformatskaya, I. I., Podobaev, A. N., and Ashcheulova, I. I., 2006, "Corrosion Resistance of Bimetals With Cladding Stainless Steel Layers in Nearly Neutral Aqueous Media," Prot. Metals, **42**(6), pp. 521–525.
[31] Qingsong, D., Dezhi, Z., Bin, Y., Zhi, Z., and Liming, H., 2008, "Finite-Element Simulation on Plastic Forming of Bimetal Composite Pipe," Natural Gas Ind., **28**(9), pp. 64–66.
[32] Peng, W., Xianghuai, D., and Lijun, F., 2009, "Rapid Finite Element Analysis of Bulk Metal Forming Process Based on Deformation Theory," Int. J. Iron Steel Res., **16**(5), pp. 23–28.
[33] Xuesheng, W., Ruzhu, W., and Peining, L., 2004, "Estimation of Residual Contact Pressures in CRA-Lined Pipe Manufactured by Hydroforming Process," China Mech. Eng., **15**(8), pp. 662–665.
[34] Dezhi, Z., 2007, "Theoretical and Experimental Study of Hydraulic Forming Process for Bimetal-Pipe," Ph.D. thesis, Southwest Petroleum University, Sichuan, China.
[35] American Petroleum Institute, 1998, "Specification for CRA Clad or Lined Steel Pipe," *API Specification 5LD*, 2nd ed., Washington, DC